

# Demonstration of 20 nm half-pitch spatial resolution with soft x-ray microscopy

W. Chao<sup>a)</sup>

Center for X-ray Optics, Lawrence Berkeley National Laboratory and Department of Electrical Engineering and Computer Sciences, University of California, Berkeley, California 94720

E. H. Anderson, G. Denbeaux, B. Harteneck, A. L. Pearson, D. Olynick, and F. Salmassi

Center for X-ray Optics, Lawrence Berkeley National Laboratory, Berkeley, California 94720

C. Song

National Center for Electron Microscopy, Lawrence Berkeley National Laboratory, Berkeley, California 94720

D. Attwood

Center for X-ray Optics, Lawrence Berkeley National Laboratory and Department of Electrical Engineering and Computer Sciences, University of California, Berkeley, California 94720

(Received 9 July 2003; accepted 25 August 2003; published 10 December 2003)

The full field, transmission soft x-ray microscope XM-1 is a valuable imaging instrument for many scientific and technological areas involving nanometer features. Operating from 300 to 1800 eV, it combines high spatial resolution, elemental discrimination, magnetic sensitivity, and a capability of imaging in various experimental conditions, such as with applied magnetic fields and electric currents. In this article, we report experiments that enable accurate spatial resolution measurement, using a new type of test pattern, made from thinned multilayer coatings. The resolution of the microscope was measured to be 20 nm, using this method. © 2003 American Vacuum Society. [DOI: 10.1116/1.1619956]

## I. INTRODUCTION

The soft x-ray transmission microscope XM-1,<sup>1,2</sup> located at Lawrence Berkeley National Laboratory (LBNL) Advanced Light Source<sup>3</sup> (ALS) synchrotron, has been successfully used to study wet biological and environmental samples,<sup>4-7</sup> nanomagnetic systems,<sup>8-10</sup> and electromigration in advanced microprocessors.<sup>11</sup> It provides a unique combination of capabilities: (1) high spatial resolution, (2) large elemental<sup>12</sup> and magnetic<sup>8</sup> contrast, based on atomic resonances, (3) large permissible sample thickness ( $\sim 0.1 \mu\text{m}$  for magnetic samples,  $\sim 10 \mu\text{m}$  for biological, environmental, and interconnect specimens), (4) *in situ* imaging in various conditions (e.g., applied magnetic field, elevated temperature, and electric current), and (5) short exposures (a few seconds) and high throughput (up to 1000 images/day). These features<sup>13</sup> complement those of other nanometer-scale imaging tools, such as electron microscopes and scanning probe microscopes. In this article, a new characterization method is described for accurate measurement of spatial resolution and the experimental results of the soft x-ray microscope are presented.

## II. SOFT X-RAY MICROSCOPE

The soft x-ray microscope XM-1 is composed of a source, a condenser lens, an objective lens, and a detector (Fig. 1). Bend magnet<sup>12</sup> radiation is used to illuminate the sample with soft x rays, allowing the microscope to operate from

300 to 1800 eV ( $\lambda = 4-0.6 \text{ nm}$ ). Linearly or elliptically polarized illumination can be obtained from in-plane or out-of-plane (electron orbit) radiation, respectively.<sup>14</sup> Collecting the radiation, the condenser lens projects a suitable illumination for the sample, and the objective lens images the sample on a detector. Both lenses are Fresnel zone plates.<sup>12</sup> Currently this type of lens offers the best spatial resolution in the soft x-ray region. The condenser zone plate (CZP) and the “micro” zone plate (MZP) that acts as an objective lens (Fig. 1) are fabricated in-house using a 100 keV electron beam lithography tool, the “Nanowriter.”<sup>15</sup> The tool has an excellent zone placement accuracy ( $< 6 \text{ nm}$ ) and circularity, achieved by using its digital pattern generator optimized for curvilinear shapes<sup>16</sup> and by its high distortion calibration accuracy ( $< 2 \text{ nm}$ ). This precision is critical to reduce aberrations, which are caused by phase errors across a zone plate’s diameter.<sup>17</sup> For the objective MZP, the bilayer resist process,<sup>18</sup> in which the zone plate is formed by electroplating a mold composed of 40 nm thick hydrogensilsequioxane and

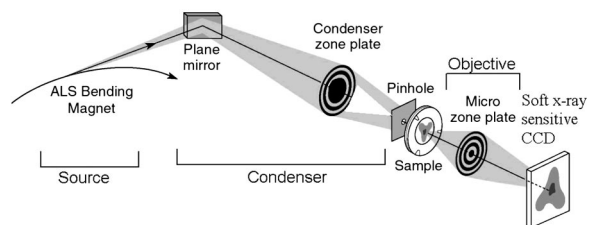


FIG. 1. Schematic diagram of the soft x-ray microscope XM-1 at LBNL’s ALS. It provides a unique set of capabilities that complement other types of high-resolution microscopes.

<sup>a)</sup>Author to whom correspondence should be addressed; electronic mail: wlchao@lbl.gov.

a layer of hard baked deep ultraviolet resist AZPN114, is used. The process yields both a small outermost zone width ( $\Delta r_{MZP}$ ) for large numerical aperture [ $NA_i = \lambda / (2\Delta r_{MZP})$ ] and a high aspect ratio for reasonable diffraction efficiency. Both the micro and condenser zone plates are fabricated on 100 nm thick, nonstoichiometric silicon nitride square membrane windows; 70  $\mu\text{m}$  in size (MZP), and 10 mm divided into four quadrants by a silicon cross support frame (CZP). The measurements reported here were obtained using CZP and MZPs with the following parameters: MZP:  $\Delta r_{MZP} = 25$  nm, 300 zones, 30  $\mu\text{m}$  diam, 80 nm thick Ni; CZP:  $\Delta r_{CZP} = 60$  nm, 41 700 zones, 10 mm diam, 120 nm thick Ni.

The microscope has a spectral resolution,  $\lambda/\Delta\lambda$ , of around 500, over the 10- $\mu\text{m}$ -diam field of view.<sup>2</sup> This is accomplished by installing a central stop of 5 mm diam on the CZP and a pinhole of a few  $\mu\text{m}$  about 100  $\mu\text{m}$  from the sample plane, forming a linear monochromator. Images are recorded by a back-thinned, soft x-ray-sensitive charge coupled device camera with a 1024 $\times$ 1024 pixel array. With an imaging magnification of 6000 as used here, each square pixel has a projected size of 4 nm at the sample.

### III. PARTIALLY COHERENT IMAGE FORMATION AND RESOLUTION TEST PATTERN DEVELOPMENT

The resolution of an imaging system, expressed as  $k\lambda/NA_i = 2k\Delta r_{MZP}$  (for zone plates), is determined by the wavelength, the numerical aperture  $NA_i$ , aberrations in the objective lens, and also, by the coherence of sample illumination. It is defined here as the half period at which the image has 26.5% modulation, the value used in the Rayleigh criteria. The effect of illumination's spatial coherence on the resolution is determined by the angular distribution of the illumination relative to the acceptance angle of the objective lens.<sup>19</sup> The parameter called the degree of partial coherence,<sup>20</sup>  $\sigma$ , equal to the ratio of the numerical aperture of the condenser ( $NA_c$ ) to that of the objective lens ( $NA_i$ ), is used for quantification:

$$\sigma = \frac{NA_c}{NA_i} = \frac{\Delta r_{MZP}}{\Delta r_{CZP}}.$$

In coherent imaging, in which a plane wave illuminates the sample,  $NA_c$  and  $\sigma$  are equal to zero. For incoherent illumination, the NA of the condenser is infinitely large relative to that of the objective, and  $\sigma$  equals infinity. Calculations show that, for illumination systems with  $\sigma$  larger than zero, the image modulation remains above 26.5% for  $k$  in a diffraction limit less than 0.5 (i.e., resolution  $< 0.5 \lambda/NA_i = \Delta r_{MZP}$ ), and the achievable resolution is smaller than  $\Delta r_{MZP}$ . For the microscope setup used here, the CZP and central stop setup has a hollow-cone illumination with  $\sigma$  equal to 25 nm/60 nm = 0.42, and a "cutout" due to the stop of 0.21.

Isolated objects, like single lines, cannot fully quantify the resolution of the microscope. To accurately measure the resolution, a test pattern consisting of high quality dense features with half periods smaller than the ultimate resolution are

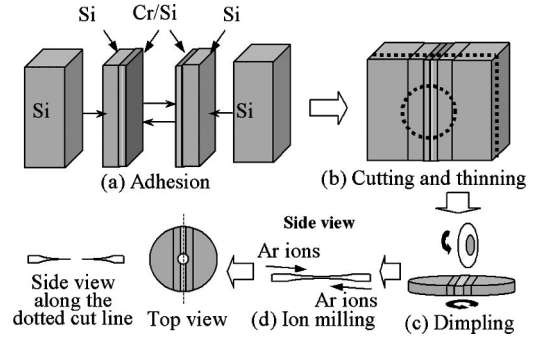


FIG. 2. Multilayer test pattern preparation. (a)–(c) A test pattern block, formed by sandwiching two pieces of Cr/Si multilayer coatings by Si blocks, was cut and thinned to create a circular disk. A concave impression was then made on each side of the disk by means of dimpling. (d) The impressions were polished using ion milling until the thinnest portion had an opening. The test pattern has a wedge-shaped thickness profile, typically between 0 and 200 nm.

desired. The pattern needs to possess good material contrast in the soft x-ray region. Periodic line and space patterns and "elbows" which allow simultaneous resolution measurement in two orthogonal directions have been fabricated in the past using the Nanowriter.<sup>21</sup> As the MZP is already fabricated with the finest lithographic lines, the test patterns cannot easily be made smaller than  $\Delta r_{MZP}$ . To fully test the microscope, a characterization method using multilayer coatings viewed in cross section was developed.

Well-defined bilayer pairs of multilayer coatings can be fabricated with magnetron sputtering<sup>22</sup> with half periods as small as 5 nm.<sup>23</sup> A variety of multilayer material pairs are available to meet the specific needs of resolution tests, such as material contrast at a given photon energy. Using sample preparation techniques developed for transmission electron microscopy (TEM), we have created thin multilayer based test patterns well suited for microscope resolution measurement.

### IV. SPATIAL RESOLUTION CHARACTERIZATION

For these first resolution tests described below, multilayer coatings composed of 40 chromium/silicon bilayer pairs, with periods of 30, 40, and 50 nm were chosen. The coatings were deposited on 500  $\mu\text{m}$  thick silicon wafers by an in-house magnetron sputtering system. The sputtering argon pressure was 1.0 mTorr and the wafers were 1.5 in. from the sputtered targets. Using an angular reflectivity scan with Cu  $K_\alpha$  x rays ( $\lambda = 1.54 \text{ \AA}$ ) at grazing incidence, their periods were measured to be 30.1, 39.0, and 48.6 nm, respectively, with errors of  $\pm 0.3$  nm. The samples were processed with conventional TEM preparation techniques<sup>24</sup> to have sufficient transparency for imaging. As shown in Figs. 2(a) and 2(b), two pieces of multilayer coatings were formed into a circular disk using mechanical (diamond and slurry disk) cutting and polishing. A "dimple" was then spherically polished into each side where individual layers could be seen [Fig. 2(c)]. The thinnest portion at the center was about 20  $\mu\text{m}$  thick. This residual thickness was removed by ion mill-

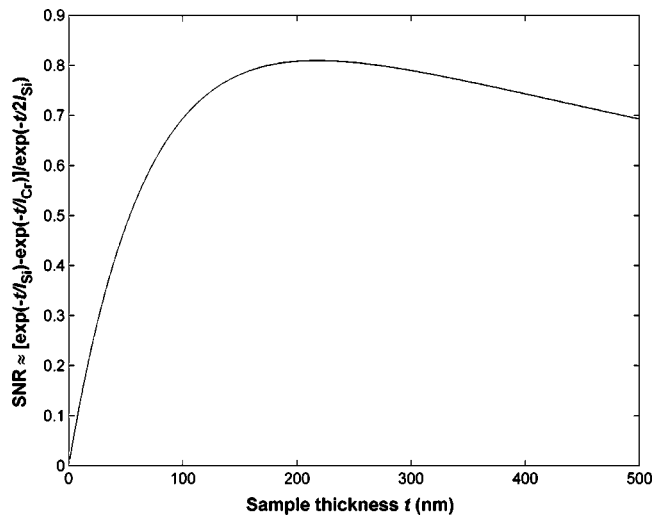


FIG. 3. Imaging signal-to-noise ratio (SNR), approximated by the differential transmission between Si (absorption length  $l_{Si}$ ) and Cr (absorption length  $l_{Cr}$ ) divided by the square root of the transmission of Si, which is more transparent, is calculated for varying sample thickness  $t$ . The optimal thickness is 217 nm.

ing at low angles ( $8^\circ$ – $10^\circ$ ) [Fig. 2(d)], until the center opened. The test pattern thus had a shallow wedge-shaped thickness profile (typically, from zero thickness to  $200\ \mu\text{m}$ ), capable of accommodating different transparency needs for imaging and sufficiently robust to handle.

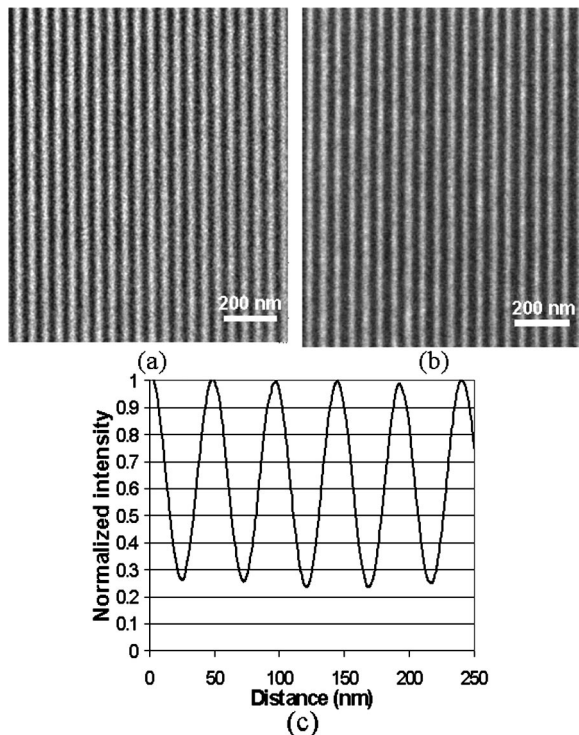


FIG. 4. (a) Soft x-ray image of the 24.3 nm half-period multilayer test pattern, taken at 600 eV ( $\lambda = 2.07\ \text{nm}$ ). Multiple images of the same area were taken to improve the SNR for modulation analysis. (b) SEM micrograph of the pattern. The micrograph and the x-ray image have 4 nm pixels. (c) A column averaged lineout of combined soft x-ray images. It shows a modulation  $((I_{\max} - I_{\min})/I_{\max})$  of 73%–76%.

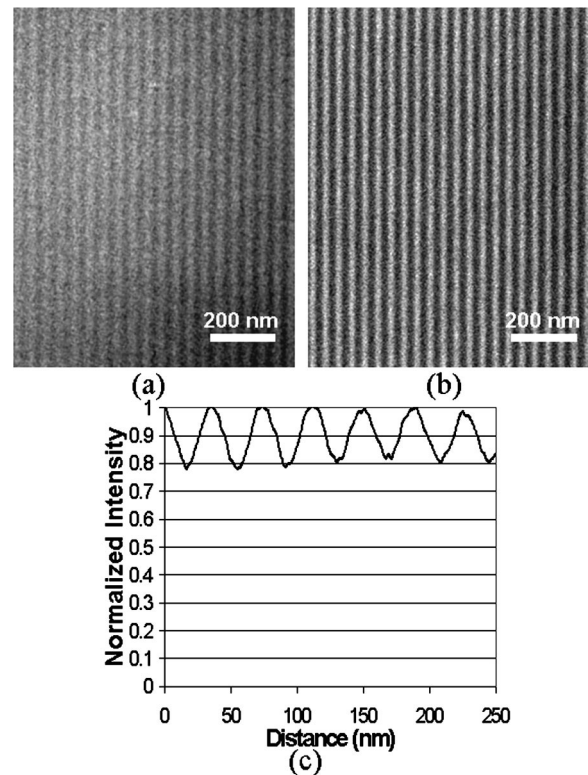


FIG. 5. (a) Soft x-ray image of the 19.5 nm half-period multilayer test pattern taken at 600 eV ( $\lambda = 2.07\ \text{nm}$ ). (b) SEM micrograph of the pattern. The pixel sizes of the micrograph and x-ray image are 4 nm. (c) Column averaged lineout of the soft x-ray images shows a modulation of 20%.

A photon energy of 600 eV ( $\lambda = 2.07\ \text{nm}$ ), just above the Cr  $L_2$  absorption edge, was selected for good material contrast in testing the microscope with these test patterns. The optimal thickness for imaging contrast, modeled by the ratio of differential transmission between Si and Cr to photon noise as seen in Fig. 3, was calculated to be 217 nm. At this thickness and a 600 eV photon energy, Si has transmission of 72.8%, Cr of 3.70%. Phase effects are negligible (less than  $2^\circ$ ).

Figure 4(a) shows a soft x-ray image of the 24.3 nm half-period multilayer test pattern. The image is similar in quality to the scanning electron microscope (SEM) micrograph of the pattern [Fig. 4(b)]. To obtain a lineout of the x-ray images with minimal noise, multiple x-ray images were combined and averaged along the pattern. The resultant lineout, shown in Fig. 4(c), exhibits a normalized modulation of 75%. Figures 5(a) and 5(b) show a soft x-ray image and a SEM micrograph of a test pattern with a measured half period of 19.5 nm. The normalized measured modulation, seen in Fig. 5(c), of the soft x-ray images of the pattern is 20%. Comparing the photon flux measured at the silicon substrates adjacent to the test patterns and the openings at the samples' centers, the thickness of the 24.3 and 19.5 nm half-period patterns was determined to be 200 nm. A 15.1 nm half-period test pattern was also imaged with the microscope, but was beyond the current system's resolution limit.

The three measured data points and a calculated image modulation curve for the microscope are shown in Fig. 6.



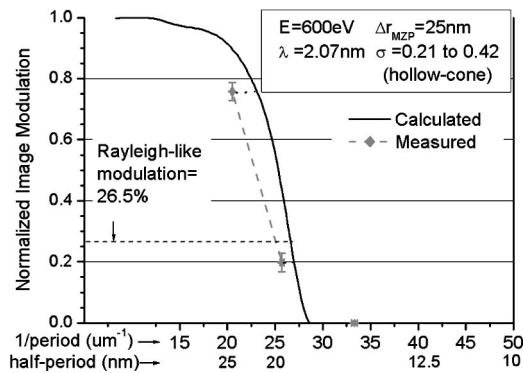


FIG. 6. Simulated image modulations for XM-1 with a hollow-cone, partially coherent illumination, and measured modulations at half periods of 24.3, 19.5, and 15.1 nm. The calculated resolution is 19 nm. A straight line through the two data points at 19.5 and 24.3 nm half periods shows that XM-1 has a resolution of 20 nm, or  $1.1\times$  diffraction-limited performance.

The calculation was performed using the SPLAT computer program,<sup>25</sup> which evaluates the Hopkins theory of partially coherent imaging<sup>19,20</sup> for desired objects and the microscope's transmission cross coefficient using numerical integration (adaptive quadrature). In this case, the objects used were periodic, equal lines and spaces. A rectangular transmission profile was assumed and interdiffusion between silicon and chromium layers was not modeled. The calculation assumed monochromatic, hollow-cone radiation, uniformly illuminating the object. The calculated modulations at 24.3 and 19.5 nm half periods are 89% and 43%, respectively. Computation shows, however, that the calculations are sensitive to the transmission profiles of the test patterns, such as line to space ratios.

Using a straight-line approximation between the measured points at 19.5 and 24.3 nm half periods, the Rayleigh-like modulation of 26.5% occurs at a half period of 20 nm, while the calculated curve achieves this modulation at 19 nm. Based on these comparisons, we conclude that the spatial resolution of the microscope is 20 nm, and thus the system is  $1.1\times$  diffraction limited at this photon energy. Further experiments and simulations, including modeling the transmission profiles of the patterns and the effects of chromaticity and polarization, will be used to investigate the imperfections.

## V. CONCLUSIONS

The spatial resolution of the soft x-ray microscope XM-1, a valuable imaging tool in nanometer studies, was measured

to be 20 nm. With the ongoing improvement of the zone plate fabrication process and better understanding of the error sources in this experiment, we anticipate extending the microscope's resolution to structures smaller than 20 nm.

## ACKNOWLEDGMENTS

The authors would like to thank Peter Fischer, for his valuable inputs, and Velimir Radmilovic and Eric Stach (NCEM/LBNL), for assistance in the test sample preparation. This work was supported by the Director, Office of Science, Office of Basic Energy Sciences, of the U.S. Department of Energy under Contract No. DE-AC03-76SF00098, and also by the Assistant Secretary for Energy Efficiency and Renewable Energy, Office of Building Technology, State, and Community Programs, of the U.S. Department of Energy under Contract No. DE-AC03-76SF00098.

- <sup>1</sup>W. Meyer-Ilse *et al.*, *Synchrotron Radiat. News* **8**, 22 (1995).
- <sup>2</sup>G. Denbeaux *et al.*, *Nucl. Instrum. Methods Phys. Res. A* **467–468**, 841 (2001).
- <sup>3</sup>N. Smith, *Phys. Today* **54(1)**, 29 (2001) ([www.als.lbl.gov](http://www.als.lbl.gov))
- <sup>4</sup>W. Meyer-Ilse *et al.*, *J. Microsc.* **201**, 395 (2001).
- <sup>5</sup>C. Larabell and M. A. Le Gros, *Mol. Biol. Cell* (submitted).
- <sup>6</sup>S. C. B. Myneni *et al.*, *Science* **286**, 1335 (1999).
- <sup>7</sup>K. E. Kurtis *et al.*, *Corros. Sci.* **42**, 1327 (2000).
- <sup>8</sup>P. Fischer *et al.*, *J. Phys. D* **35**, 2391 (2002).
- <sup>9</sup>G. Kusinski *et al.*, *J. Appl. Phys.* **91**, 7541 (2002).
- <sup>10</sup>G. Denbeaux *et al.*, *J. Phys. IV* **104**, 477 (2003).
- <sup>11</sup>G. Schneider *et al.*, *J. Vac. Sci. Technol. B* **20**, 3089 (2002).
- <sup>12</sup>D. Attwood, *Soft X-rays and Extreme Ultraviolet Radiation* (Cambridge University Press, Cambridge, U.K., 1999).
- <sup>13</sup>G. Denbeaux *et al.*, *Synchrotron Radiat. News* **16**, 16 (2003).
- <sup>14</sup>K. J. Kim, *Opt. Eng. (Bellingham)* **34**, 342 (1995).
- <sup>15</sup>E. H. Anderson *et al.*, *J. Vac. Sci. Technol. B* **18**, 2970 (2000).
- <sup>16</sup>E. H. Anderson *et al.*, *J. Vac. Sci. Technol. B* **13**, 2529 (1995).
- <sup>17</sup>For minimal aberration, the zone placement error should be limited to one-third of the smallest zone width.
- <sup>18</sup>D. L. Olynick *et al.*, *J. Vac. Sci. Technol. B* **19**, 2896 (2001).
- <sup>19</sup>J. Goodman, *Statistical Optics* (Wiley, New York, 2000), pp. 303–324.
- <sup>20</sup>M. Born and E. Wolf, *Principles of Optics* (Cambridge University Press, New York, 1999), pp. 441, 596–606 (the book uses  $m$  instead of  $\sigma$  to denote the degree of partial coherence).
- <sup>21</sup>W. Chao *et al.*, *Proc. SPIE* **4146**, 171 (2000).
- <sup>22</sup>J. H. Underwood, E. M. Gullikson, and K. Nguyen, *Appl. Opt.* **32**, 6985 (1993).
- <sup>23</sup>T. W. Barbee, S. Mrowka, and M. C. Hettrick, *Appl. Opt.* **24**, 883 (1985) (see [www.cxro.lbl.gov/multilayer/survey.html](http://www.cxro.lbl.gov/multilayer/survey.html)) for current half periods achieved and different multilayer material pairs).
- <sup>24</sup>J. C. Bravman and R. Sinclair, *J. Electron Microsc. Tech.* **1**, 53 (1984).
- <sup>25</sup>K. K. H. Toh and A. R. Neureuther, *Proc. SPIE* **772**, 202 (1987).